MULTIPARTICLE PRODUCTION IN DEEP INELASTIC LEPTON SCATTERING AND SOFT PROTON PROTON COLLISIONS*,**

By K. Werner

Brookhaven National Laboratory, Upton NY 11973, USA

(Received November 23, 1987)

We demonstrate how the theoretical knowledge about multiparticle production in deep inelastic lepton scattering can be incorporated into a multistring model for low p_t proton proton collisions.

PACS numbers: 12.10.Dm

1. Introduction

In the late 1960s the discovery of large p_t lepton proton scattering suggested the existence of pointlike particles inside the proton, called "partons", which turned out to be identical to quarks [1]. Because at large momentum transfer Q^2 quarks appear to be free, a theoretical description of the scattering process as a superposition of elementary electron parton diagrams was possible (Quark Parton Model [2]). An analysis of e^+e^- and deep inelastic lepton scattering data in terms of the Quark Parton Model allows the determination of momentum distributions of quarks and gluons in a fast-moving proton (structure functions). Also, the fragmentation (hadronization) of color strings, consisting of the scattered quarks and the spectator partons, can be studied.

For high energy hadron hadron scattering the situation is quite different, since most likely only a very small amount of transverse momentum is transferred. For this case asymptotic freedom of quarks and perturbative treatment do not apply. Nevertheless, successful models for low p_t hadron hadron scattering have been constructed using the

* Presented at the XXVII Cracow School of Theoretical Physics, Zakopane, Poland, June 3–15, 1987.

** This manuscript has been authored under contract number DE-AC02-CH00016 with the U.S. Department of Energy. Accordingly, the U.S. Government retains a non-exclusive, royalty-free license to publish or reproduce the published form of this contribution, or allow others to do so, for U.S. Government purposes.

knowledge from lepton scattering about the partonic substructure of the proton and about string fragmentation.

In Chapter 2 we review the Quark Parton Model for deep inelastic lepton proton scattering and demonstrate how structure and fragmentation functions are obtained from scattering data. In Chapter 3 we discuss a phenomenological model on string fragmentation based on the Field-Feynman model. We introduce in Chapter 4 a multistring model for soft proton proton scattering using a fragmentation scheme described in Chapter 3. Finally, in Chapter 5 we apply the fragmentation model as well as the proton proton model to compare with data.

2. *Deep inelastic lepton scattering*

We consider in this Chapter the scattering of electrons, muons, neutrinos or antineutrinos on nucleons with large momentum transfer involved. According to the quark parton model, the cross section for lepton proton collisions is an incoherent superposition of lepton quark scatterings where, because of the large transferred momentum, only the lowest order diagram is considered. This statement can be written as

$$\frac{d^2\sigma}{dxdy}(\mathrm{lN}) = \sum_i \int d\xi q_i(\xi) \frac{d^2\sigma}{dxdy}(lq_i), \tag{1}$$

where i represents a quark flavor, ξ is the momentum fraction of the quark in the proton, q_i is the momentum distribution of quarks with flavor i, and the dimensionless quantities x and y are defined as

$$x = \frac{-q^2}{2pq} \equiv \frac{Q^2}{2pq}, \tag{2}$$

$$y = \frac{pq}{pk}, \tag{3}$$

with k, k', q and p being the momenta of the incoming and outgoing lepton, the transferred boson, and the proton. In the laboratory system we find, because of $p = (M, 0, 0, 0)$:

$$x = \frac{Q^2}{2M(E-E')}, \tag{4}$$

$$y = \frac{E-E'}{E}, \tag{5}$$

with E and E' being the energies of the incoming and outgoing leptons. Neglecting masses, momentum conservation $(\xi p+q)^2 = 0$ leads to

$$x = \frac{-q^2}{2pq} \equiv \xi. \tag{6}$$

From Eqs (5) and (6) we conclude that the kinematical allowed region is given by

$$0 \leqslant x, y \leqslant 1.$$

In the case of electrons (or muons) scattering on nucleons, the elementary lepton quark cross section is given as

$$\frac{d^2\sigma}{dxdy}(eq_i) = \frac{2\pi\alpha^2}{Q^4} sx(1+(1-y)^2)e_i^2\delta(\xi-x). \tag{7}$$

From Eqs (7) and (1) we obtain

$$\frac{d^2\sigma}{dxdy}(eN) = \frac{2\pi\alpha^2}{Q^4} sx(1+(1-y)^2)\sum_i e_i^2 q_i(x). \tag{8}$$

In a similar fashion, using the elementary neutrino quark and neutrino antiquark cross section,

$$\frac{d^2\sigma}{dxdy}(\nu q) = \frac{G^2}{\pi} sx\delta(\xi-x), \tag{9}$$

$$\frac{d^2\sigma}{dxdy}(\nu\bar{q}) = \frac{G^2}{\pi} sx(1-y)^2\delta(\xi-x) \tag{10}$$

we find from Eq. (1) (with $\theta_c = 0$ and charm ignored):

$$\frac{d^2\sigma}{dxdy}(\nu N) = \frac{G^2}{\pi} sx(q_d(x)+(1-y)^2 q_{\bar{u}}(x)), \tag{11}$$

$$\frac{d^2\sigma}{dxdy}(\bar{\nu}N) = \frac{G^2}{\pi} sx((1-y)^2 q_u(x)+q_{\bar{d}}(x)). \tag{12}$$

Equations (8, 11, 12) show that the cross sections $d^2\sigma/dxdy(lN)$ for $l = e, \mu, \nu, \bar{\nu}$ can be expressed in terms of the quark structure functions $q(x)$. By using these equations it is possible to determine the structure functions from measured cross sections.

In order to treat inclusive particle production, we introduce the variable $z = p_{\parallel}/p_{max}$ where $p_{\parallel}$ is the longitudinal momentum of the produced hadron in the cm system of the string, and p_{max} is the maximal possible momentum. For electron (or muon) nucleon scattering the cross section for inclusive hadron production can be written (see Eq. (8)):

$$\frac{d^3\sigma}{dxdydz}(eN) = \frac{2\pi\alpha^2}{Q^4} sx(1+(1-y)^2)$$
$$\times \sum_i e_i^2 q_i(x)\{\theta(z)D^h_{q_i}(z)+\theta(-z)D^h_{p-q_i}(|z|)\}, \tag{13}$$

where the fragmentation functions $D^h_a(z)$ represent the z-distribution of hadrons originating from the jet a (this assumes that a string can be treated as two independent jets moving

into opposite directions). A similar formula holds for neutrino scattering (compare Eq. (11)):

$$\frac{d^3\sigma}{dxdydz}(\nu p) = \frac{Gsx}{\pi} q_d(x)\{\theta(z)D_u^h(z)+\theta(-z)D_{p-d}^h(|z|)\}$$

$$+\frac{Gsx}{\pi}(1-y)^2 q_{\bar{u}}(x)\{\theta(z)D_{\bar{d}}^h(z)+\theta(-z)D_{p-\bar{u}}^h(|z|)\}. \tag{14}$$

A corresponding formula holds for $\bar{\nu}p$ scattering. If sea quarks can be neglected (which is justified for certain experimental cuts) we find

$$\frac{d^3\sigma}{dxdydz}(\nu p) = \frac{Gsx}{\pi} q_d(x)\{\theta(z)D_u^h(z)+\theta(-z)D_{uu}^h(|z|)\} \tag{15}$$

and

$$\frac{d^3\sigma}{dxdydz}(\bar{\nu}p) = \frac{Gsx}{\pi}(1-y)^2 q_u(x)\{\theta(z)D_{\bar{d}}^h(z)+\theta(-z)D_{ud}^h(|z|)\}. \tag{16}$$

Equations (15) and (16) tell us that for $z > 0$ the cross section is proportional to the quark fragmentation function; for $z < 0$ the cross section is proportional to diquark fragmentation. In other words, quark and diquark fragmentation functions can be measured.

3. A model for string fragmentation

Different types of models provide a phenomenological description of string fragmentation: (*i*) The Field Feynman Model [3] (FFM) where the two jets fragment independently in an iterative manner; (*ii*) the Lund model [4] where resonance production is realized through breaking the string in smaller and smaller pieces; (*iii*) Parton shower models [5] where ordered gluon radiation is the source of particle production. We shall discuss the FFM, first of all, to introduce the concept, the analytical solvable case of an infinite energy quark jet, which produces only mesons. Later, we shall generalize the model to include diquark fragmentation and baryon production.

The analytic solvable FFM is defined as follows: a quark q_i with energy e produces via quark-antiquark production a meson with energy xe, leaving back a quark with energy $(1-x)e$, which now plays the role of the original quark and produces in the same way the next meson with energy $(1-x)x'e$ etc. A so-called splitting function $f(x)$ governs the distribution of the energy fraction x of the meson relative to the jet quark. For an infinite energy jet, the energy fraction distribution $D(x)$ of produced mesons fulfills the integral equation (for one kind of flavor):

$$D(x) = f(x)+\int_x^1 d\xi f(1-\xi)D\left(\frac{x}{\xi}\right)\frac{1}{\xi}. \tag{17}$$

The term $f(x)$ on the rhs of Eq. (17) represents mesons which are produced from the original jet quark in the first fragmentation step (first rank meson). The integral in Eq. (17) counts higher rank mesons: $f(1-\xi)d\xi$ is the probability to have a remainder jet (after the first fragmentation) with energy ξe, $D(x/\xi)/\xi$ is the distribution of mesons produced from the remainder jet, renormalized to its energy ξe (rather than e of the original jet quark). The reasonable ansatz

$$f(x) = (n+1)(1-x)^n \tag{18}$$

allows an analytical solution of the integral equation, Eq. (17):

$$D(x) = \frac{f(x)}{x} \tag{19}$$

which shows the correct behavior for large x:

$$\lim_{x \to 1} D(x) = f(x). \tag{20}$$

For small values of x, ($x \ll 1$), we find

$$D(x) \approx \frac{n+1}{x}. \tag{21}$$

In the central region (small x) it is more convenient to use the rapidity variable y rather than the energy e; both are related through

$$e = \mu \cosh y, \tag{22}$$

where $\mu = (m^2+p_t^2)^{1/2}$ is the transverse mass of the meson. From Eqs (21) and (22) we conclude for the rapidity density $D(y)$, if y is not very large (comparable to y_{max} and not very small)

$$D(y) \approx n+1, \tag{23}$$

which means: the height of the rapidity distribution stays constant with energy; only the width increases linear in logs which consequently also leads to a linear increase of the mean multiplicity $\langle n \rangle$:

$$\langle n \rangle = a+b \log s. \tag{24}$$

These important features, rapidity plateau and linear increase of the mean multiplicity with logs, remain true also for the more general FFM [6] which we describe in the following. In order to treat quark and diquark fragmentation into mesons and baryons (or corresponding resonances) we need four elementary vertices (instead of the one of the analytic model) as shown in Fig. 1: (a) quark into meson leaving a quark; (b) quark into baryon leaving an antidiquark; (c) diquark into meson leaving a diquark; and (d) diquark into baryon leaving an antiquark (corresponding vertices apply for antiquark and antidiquark fragmentation).

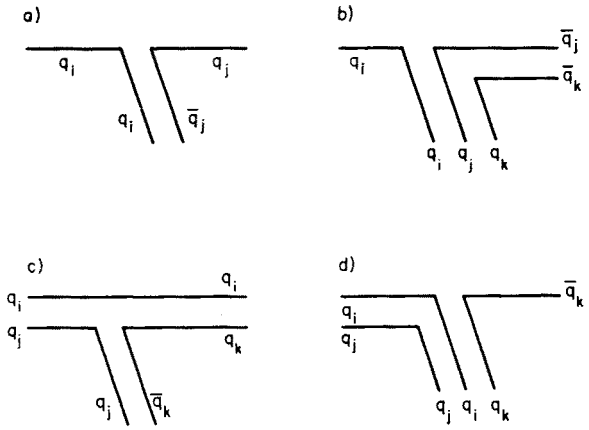

Fig. 1. The elementary fragmentation vertices for the fragmentation of quark and diquark jets (antiquark and antidiquark fragmentation is obtained by exchanging quarks and antiquarks in the figure)

The relative weights of baryon and meson production in quark jets (P_q^b, $1-P_q^b$) and in diquark jets (P_{qq}^b, $1-P_{qq}^b$) provide two free parameters. A further parameter is the probability P_s to create $s\bar{s}$ pairs in competition to $u\bar{u}$ and $d\bar{d}$ pair production; the latter two are assumed to be produced equally probable:

$$P_u = \frac{1-P_s}{2},$$

$$P_d = \frac{1-P_s}{2}. \tag{25}$$

The energy of a primary hadron relative to the energy of the corresponding jet is generated according to splitting functions $f_q^m(x)$, $f_q^b(x)$, $f_{qq}^m(x)$, and $f_{qq}^b(x)$ for the four vertices of Fig. 1. The splitting functions are a crucial input of the model: they determine momentum distributions of produced particles; moreover, the multiplicities depend strongly on these functions. Therefore, one would like to have some theoretical basis to determine them, rather than having free parameters. Indeed, there exist QCD results for the asymptotic behavior of such elementary vertices as x approaches 1: the fragmentation behaves like $(1-x)^{2n-1}$, where n counts the number of spectators (counting rules [22]). We have $n = 1$ for the vertices Fig. 1 (a, d), and $n = 2$ for the vertices Fig. 1 (b, c), leading to a large x behavior as $(1-x)^1$ and $(1-x)^3$ respectively. In order to account for the fact that one does *not* observe a rapidity plateau of baryons produced in deep inelastic scattering [7] we add a factor x^α for the case of baryon production. We eventually use (up to normalization factors)

$$\begin{aligned} f_q^m(x) &= (1-x), \\ f_q^b(x) &= x^\alpha(1-x)^3, \\ f_{qq}^m(x) &= (1-x)^3, \\ f_{qq}^b(x) &= x^\alpha(1-x). \end{aligned} \tag{26}$$

A finite transverse size R of the string requires a finite transverse momentum of the order

$$\langle p_t \rangle \approx \frac{1}{R}.$$

We generate a transverse momentum of a quark according to the exponential distribution

$$f(\vec{p}_t) = \frac{2}{\pi \langle p_t \rangle^2} e^{-2p_t/\langle p_t \rangle}. \tag{27}$$

The antiquark assumes $-\vec{p}_t$.

The jet fragmentation cascade is terminated when the jet energy is too small to produce further particles. In order to achieve flavor conservation (and thus baryon number conservation) we combine the two remaining partons of two corresponding jets to make a primary hadron. The last fragmentation step before the recombination is performed only if the sum of the masses of all produced particles, including the recombined one, is smaller than the string mass M. We achieve approximate energy conservation. Using this prescription to conserve flavor and energy, we no longer have a really independent fragmentation scheme.

Actual calculations are carried out on Monte Carlo basis, which allows to treat cutoffs in a proper way and which allows in particular to calculate much more than only inclusive results as shown in the analytic model. Results will be presented in Chapter 5.

4. Multistring model for soft proton proton scattering

The theoretical treatment of low p_t proton proton scattering is much less straightforward than deep inelastic lepton scattering, since the small momentum transfer prohibits perturbative treatment. Nevertheless, we want to use the concept of color strings, which we studied in the previous chapter on lepton scattering, also to describe proton proton scattering.

The main assumption of the proton model is: the whole process can be divided into two steps, formation of strings and subsequent string fragmentation. The hadronization time being much larger than the reaction time justifies this assumption. The fragmentation is treated as described in Chapter 3, even using the same parameters used to describe lepton proton scattering data. In the following, we give a prescription of how to form strings in a proton proton collision. The model is similar to Dual Parton models [8–11], yet more predictive than HILUND [12] and ISAJET [13].

Color exchange is assumed to cause the formation of color strings: i exchanges of color between quarks of the projectile and target proton result in $2i$ strings. The relative weight of a i color exchange contribution is named w_i, thus cross sections can be written as

$$\sigma = \sum_{i=1}^{\infty} w_i \sigma_i, \tag{28}$$

σ_i being the contribution consisting of $2i$ strings. We first describe the dominant $i = 1$ contribution, i.e. the formation of two strings: color exchange between a quark of the

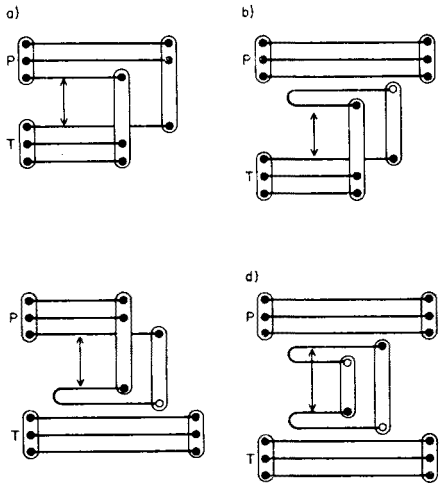

Fig. 2. The four basic (one-color exchange) contributions to pp collisions. Color exchange (arrow) is the basic mechanism to rearrange color singlets (closed lines) and thus to produce strings. The contributions a) to d) differ in the number N of quarks being part of a white $q\bar{q}$ pair: $N = 0$ for a), $N = 1$ for b), c), and $N = 2$ for d)

projectile and a quark of the target rearranges the color structure of the pp system: instead of two protons in singlet states we find two singlets each consisting of a diquark and a quark of the other nucleon (see Fig. 2a). We explicitly treat the case in which one (or both) of the quarks participating in the color exchange is accompanied by an antiquark such that the $q\bar{q}$ pair is color neutral, because in this case the diquark quark $(qq-q)$ string is replaced by a $q-\bar{q}$ string and a baryon. In Figs 2b, c, d we show this for the case when the projectile quark (b), the target quark (c), of both quarks (d) are part of colorless $q\bar{q}$ pairs. We generate quarks with and without $\bar{q}$ partners with probabilities w and $1-w$, so the relative weights of the contributions 1a, b, c, d can be expressed in terms of the parameter w (in a complicated way because certain events have to be discarded as unphysical). So far, we treat neither color exchange between antiquarks nor color exchange between gluons. Gluons are only spectators, in the sense that diquarks are implicitly assumed to be "dressed", i.e. to contain gluons.

Looking at figures 2a and 2d indicates already a possible generalization: the color exchange between quarks being part of white $q\bar{q}$ pairs (1d) may occur in addition to the nondiffractive color exchange of Fig. 2a leading to a $i = 2$ (two-color exchanges) contribution with $2i = 4$ strings. Two color exchanges of the type 2d in addition to the exchange of type 2a leads to a $i = 3$ contribution with six strings and so on. The same generalizations apply to the contributions 2b, 2c, and 2d. This expansion in terms of the number of color exchanges (i.e. in terms of the number of strings) corresponds to the multi-Pomeron exchange picture of Abramovskii, Kancheli and Gribov [14] and is also used by other authors (Ref. [10] and Refs therein).

How do we determine energy and momentum (and so the mass) of a string? We want to choose a frame in which both protons are fast and moving in opposite directions, so

we take the pp cm system. As discussed in Section 2, the distribution of the momentum fraction of a parton i in a fast-moving proton, the so-called quark structure functions $q_i(x)$, can be determined from deep inelastic lepton scattering data. (For a parametrization see Ref. [15]). We generate flavor and energy of the quarks involved in the color exchange and of the antiquarks according to the structure functions. The distribution functions $q_i(x)$ also determine the relative weight of valence and sea quarks, yet in the case of a quark accompanied by an antiquark we always assume the quark to be a sea quark and the pair to be flavor white (some further study of pp → nX, for example, is necessary to justify or reject this last assumption). By energy conservation, the energy fraction of a diquark is $1-x$ when the quark has energy fraction x. (For reasons discussed below, we take x to be the energy rather than the momentum fraction, which amounts to the same for large x.)

What about transverse momenta? Since the partons are confined to the proton size R, the uncertainty principle requires a finite transverse momentum of the order

$$\langle p_t \rangle \approx \frac{1}{R} . \tag{29}$$

We generate transverse momenta for the quarks according to the exponential distribution

$$f(\vec{p}_t) = \frac{2}{\pi \langle p_t \rangle^2} e^{-\frac{2p_t}{\langle p_t \rangle}} . \tag{30}$$

To preserve momentum, the diquark corresponding to a quark with momentum $\vec{p}_t$ assumes a transverse momentum of $-\vec{p}_t$. The strings are now fully determined, since we assume the string constituents (quarks, antiquarks, and diquarks) to be massless.

The invariant mass of a qq−q string consisting of a diquark with momentum $(1-x_2)p$ and a quark with momentum $x_1 p$, is for $\langle p_t \rangle = 0$ given as

$$M^2 = 4x_1(1-x_2)p^2. \tag{31}$$

This shows that for $\langle p_t \rangle = 0$ the infrared divergence of the sea quark structure functions ($q_{sea}(x) \sim x^{-1}$) raises no problems, because for $x \to 0$ the string mass vanishes, and this event does not count (we discard events including qq−q string with masses less than the proton mass and q−$\bar{q}$ string with masses less than the pion mass). For finite $\langle p_t \rangle$ we have the unphysical situation of infinitely many sea quarks with very small $p_\parallel$ but finite p_t, and thus finite energy — if the variable x occurring in the structure functions is longitudinal momentum fraction. Therefore, we take x to be the energy fraction which solves this problem, and for larger values of x energy and longitudinal momentum are equivalent (one could also take the light cone variable p_+ rather than the energy).

5. *Results*

Before comparing Monte Carlo results with experimental data, we want to discuss the parameters. The probability P_s to create a s$\bar{s}$ during fragmentation is taken to be $P_s = 0.14$ from Ref. [13]. We fix the baryon production probabilities P_q^b and P_{qq}^b as well

as the splitting function parameter α by comparing with EMC data [16] on proton production in deep inelastic μp scattering. We obtain best agreement for $P_q^b = 0.12$, $P_{qq}^b = 0.75$, and $\alpha = 1.5$. The mean transverse momentum of produced $q\bar{q}$ pairs as well as the mean transverse momentum of partons in protons assumes $\langle p_t \rangle = 0.5$ GeV. For the momentum transfer Q^2 entering the quark structure functions, we use $Q^2 = 4\,\text{GeV}^2$, which is the smallest value of Q^2 where the parametrizations of Ref. [15] are valid. The probability w, that in a pp collision an interacting quark is accompanied by an antiquark, is fixed such that the fraction of events involving one such $q\bar{q}$ pair matches the ratio $\sigma_{\text{diffr}}/\sigma_{\text{inel}}$, which has, over a wide energy range, the value 0.2 [17]. This prescription is explained in Ref. [18]. The multicolor exchange probability w_i entering Eq. (28) provides in principle an infinite number of parameters. On the other hand, the results we will discuss in this paper are rather insensitive to higher than the first moment

$$\langle i \rangle = \sum_{i=1}^{\infty} i w_i \tag{32}$$

of w_i, and this first moment is fixed to give the correct mean multiplicity ($\langle i \rangle$ increases with energy). In the actual calculations we use an exponential distribution

$$w_i = \frac{1}{\langle i \rangle} \left(\frac{\langle i \rangle - 1}{\langle i \rangle} \right)^i, \tag{33}$$

using instead a Poisson distribution for w_i leads to quite similar results.

In the following we compare Monte Carlo results with data. In all plots we use the convention: open dots are data, full dots are Monte Carlo results, and lines may be either of them. In Fig. 3 we compare $\bar{\nu}p$ scattering data [19] with ud−d string fragmentation results. The variable x is the momentum fraction of the produced particle relative to the maximum possible momentum, which results in

$$x = \frac{2p_{\text{hadr}}}{\sqrt{s}}$$

for a large string mass $\sqrt{s}$. The Monte Carlo results are real predictions; no free parameters have been adjusted to produce these curves. The significant difference between fragmentation of d-quarks into π^- and into π^+ is due to the fact that a π^- can be produced in one fragmentation step, whereas a π^+ requires either two fragmentation steps or a resonance decay (we have elementary vertices only for "favored" hadron production; the produced hadron always contains a jet parton!). The experimental fragmentation functions for the fragmentation of d-quarks into pions as shown in Fig. 4 are obtained from μp data [16] assuming that there exist only two kinds of fragmentation functions for pions produced from quarks: "favored" ones, where the meson contains the quark, and "unfavored" ones, where the quark is not contained in the meson. Next we show some proton proton results. In Fig. 5 we display the distribution of the rapidity y, defined as

$$y = \tfrac{1}{2} \log \frac{e + p_\parallel}{e - p_\parallel}$$

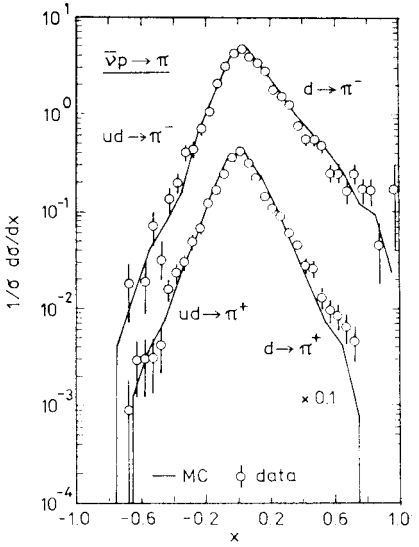

Fig. 3. Longitudinal momentum distributions of π^- (upper curve) and π^+ (lower curve) produced in $\bar{\nu}p$ collisions which is (for this experiment) equivalent to ud−d string fragmentation. The average squared energy is $\langle W^2 \rangle = 6.2^2\ \mathrm{GeV}^2$. The variable x is the longitudinal momentum fraction relative to the maximal possible momentum for this kind of fragmentation. Positive x is quark fragmentation; negative x is diquark fragmentation

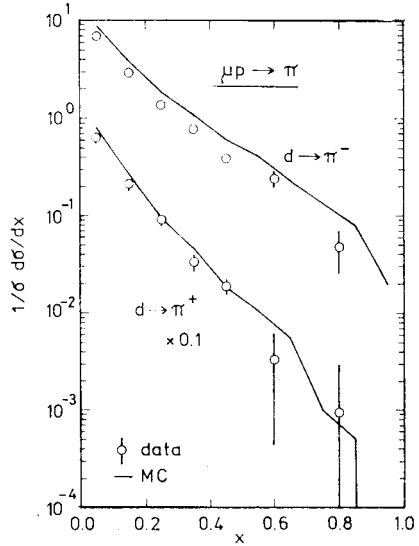

Fig. 4. Longitudinal momentum distribution of π^- (upper curve) and π^+ (lower curve) originating from d quark fragmentation (def of x, see Fig. 4). The data points are extracted from μp scattering with $\langle W^2 \rangle = 11.4^2\ \mathrm{GeV}^2$

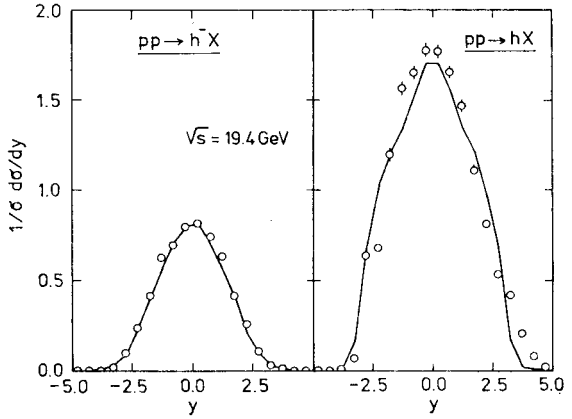

Fig. 5. Rapidity distribution for negative (left) and charged (right) particles for a pp collision at 200 GeV Data (points) from Ref. [23]

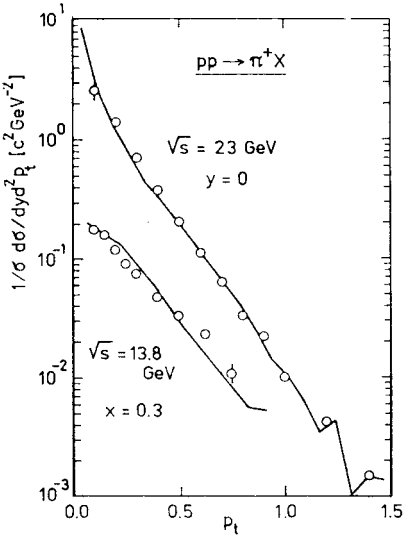

Fig. 6. Transverse momentum distribution of pions in the central region ($y = 0$) and in the projectile fragmentation region ($x = 0.3$) for a pp collision at 280 GeV and 100 GeV. Data (points) from Refs [24, 25]

for negative particles (left) and for charged particles (right). The transverse momentum p_t is integrated out. One should keep in mind, at least for the charged particle distribution, that the experimental error bars are larger than indicated, which can be concluded from the asymmetric shape of the distribution (the theoretical curve is rather symmetric, as it should be). Figure 6 shows the transverse momentum (p_t) distribution of pions in the central region ($y = 0$), and in the projectile fragmentation region ($x = 0.3$). In Fig. 7 we show the p_t distribution of protons at $x = 0.3$ and at $x = 0.92$. In Fig. 8 finally we display multiplicity distributions. It is known for many years already [20] that multiplicity distribu-

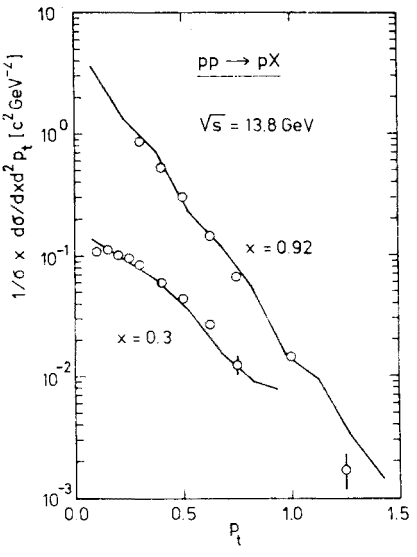

Fig. 7

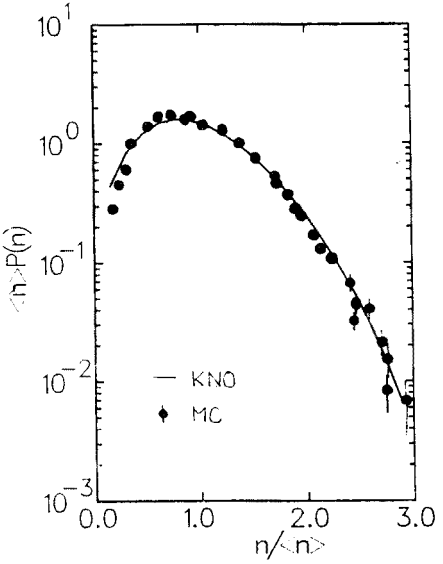

Fig. 8

Fig. 7. Transverse momentum distribution of protons at $x = 0.3$ and $x = 0.92$ for a pp collision at 100 GeV• Data (points) from Ref. [25]

Fig. 8. Multiplicity distributions for pp collisions at 14, 23, and 53 GeV compared to the KNO function of Ref. [21]

tions $P(n)$ for pp collisions in a wide energy range scale, i.e..

$$\langle n\rangle P(n) = \Psi\left(\frac{n}{\langle n\rangle}\right)$$

with a universal energy independent function Ψ. The curve in Fig. 8 represents the parametrization of Ψ according to Ref. [21]. The Monte Carlo results for pp collisions with cm energies of 14, 23, and 53 GeV are very close to the experimental curve.

6. *Conclusion and outlook*

We have demonstrated that it is possible to construct a model for low p_t proton proton collisions in the spirit of the Quark Parton Model, originally designed to describe high p_t processes in deep inelastic lepton scattering. The assumption that strings produced in soft pp collisions fragment in the same way as strings from deep inelastic lepton scattering is by far not trivial. Nevertheless, using this assumption, many pp data can be reproduced similarly well as lepton proton data. Very few additional parameters enter the pp model, and since a huge variety of pp data exist (covering a wide energy range) it is possible to make sensible tests of the model to confirm or reject the proposed reaction mechanism. Some confidence into a proton proton model is in particular necessary to extrapolate the pp model in order to design proton nucleus or nucleus nucleus models. Such models for

ultrarelativistic nucleus nucleus collision have attracted considerable interest in the last few years in connection with the search for a quark gluon phase transition in these collisions. A solid understanding of the bulk of all nucleus nucleus collisions would help to detect such a (probably) rare transition event.

I acknowledge helpful discussions with P. Aurenche, A. Białas, B. Buschbeck, A. Capella, M. Kutschera, and P. Lipa. This work has been supported by the U. S. Department of Energy under contract no. DE-AC02-76CH00016.

REFERENCES

[1] F. E. Close, *An Introduction to Quarks and Partons*, Academic Press 1979.
[2] P. D. P. Collins, A. D. Martin, *Rep. Prog. Phys.* **45**, 335 (1982).
[3] R. D. Field, R. P. Feynman, *Nucl. Phys.* **B136**, 1 (1978).
[4] B. Anderson, G. Gustafson, G. Ingelman, T. Sjöstrand, *Phys. Rep.* **97**, 31 (1983).
[5] G. Marchesini, B. R. Webber, *Nucl. Phys.* **B238**, 1 (1984); B. R. Webber, *Nucl. Phys.* **B238**, 492 (1984).
[6] K. Werner, BNL preprint 39726 (to be published in *Phys. Lett.* **B**).
[7] EMC; M. Arneodo et al., *Z. Phys.* **C31**, 1 (1986).
[8] A. Capella, J. Tran Thanh Van, *Z. Phys.* **C10**, 249 (1981).
[9] J. Ranft, S. Ritter, *Z. Phys.* **C27**, 413 (1985).
[10] P. Aurenche, F. W. Bopp, J. Ranft, *Z. Phys.* **C23**, 67 (1984).
[11] J. P. Pansart, in: Proc. of the Fifth International Conference on Ultra-Relativistic Nucleus-Nucleus Collision, Asilomar, eds. L. Schroeder, M. Gyulassy; *Nucl. Phys.* **A461** (1987).
[12] B. Anderson, G. Gustafson, B. Nielsson-Almquist, *Nucl. Phys.* **B281**, 289 (1987).
[13] F. E. Paige, S. D. Protopopescu, in: Proc. of the 1986 Summer Study on the Physics of the Superconducting Supercollider, 1986, pp. 320–325.
[14] V. A. Abramovskii, O. V. Kancheli, V. N. Gribov, in XVI International Conf. on High Energy Physics, Batavia IL, 1973, Vol. 1, p. 389.
[15] D. W. Duke, J. F. Owens, *Phys. Rev.* **D30**, 49 (1984).
[16] EMC; M. Arneodo et al., *Phys. Lett.* **150B**, 458 (1985).
[17] A. Wróblewski, Proc. of 14th International Symp. on Multiparticle Dynamics, Granlibakken 1983, eds. P. Yager, J. F. Gunion, World Scientific Publ. Co.
[18] K. Werner, M. Kutschera, *Phys. Lett.* **183B**, 385 (1987).
[19] P. Allen et al., *Nucl. Phys.* **B214**, 369 (1983).
[20] Z. Koba, N. B. Nielsen, P. Olesen, *Nucl. Phys.* **B40**, 317 (1970).
[21] P. Slattery, *Phys. Rev. Lett.* **29**, 1624 (1972).
[22] J. F. Gunion, Proc. of 11th International Symposium on Multiparticle Dynamics, Bruges 1980, p. 767.
[23] C. De Marzo et al., *Phys. Rev.* **D26**, 1019 (1982).
[24] B. Alper et al., *Nucl. Phys.* **B100**, 237 (1975).
[25] A. E. Brenner et al., *Phys. Rev.* **D26**, 1497 (1982).